

A comparison of the strain and the classic experimental modal analysis

Tadej Kranjc¹, Janko Slavič^{*2}, Miha Boltežar²

April 30, 2014

Cite as:

Kranjc, T., Slavič, J. and Boltežar, M., **A comparison of the strain and the classic experimental modal analysis**, Journal of Vibration and Control, published online 29 April 2014, DOI: 10.1177/1077546314533137

¹ Ydria Motors d.o.o., Podskrajnik 16, 1380 Cerknica, Slovenia-EU.

² Faculty of Mechanical Engineering, University of Ljubljana, Aškerčeva 6, 1000 Ljubljana, Slovenia-EU.

* Corresponding author: Janko Slavič, janko.slavic@fs.uni-lj.si, +386 1 4771 226

Abstract

This research is focused on a comparison of the classic and the strain Experimental Modal Analysis (EMA). The modal parameters (the natural frequencies, the Displacement Mode Shapes (DMSs) and the damping) of real structures are usually identified with the classic EMA, where the responses are measured with motion sensors (*e.g.*, accelerometers). The strain EMA is a special approach in the field of EMA, where the responses are measured with strain sensors. Classic EMA is the preferred method, but strain EMA offers advantages that are important for particular applications: for example, the direct identification of Strain Mode Shapes (SMSs), which is important in the vibration-fatigue and damage-identification models. The next advantage is that the strain EMA can sometimes be used, for experimental/geometrical reasons, where the classic EMA cannot. There are also drawbacks: *e.g.*, with strain EMA only, the mass-normalization of the DMSs and SMSs cannot be performed. This

study researches the theoretical similarities and differences of both EMA approaches. Furthermore, the accuracy of both approaches for the case of a free-free supported beam and a free-free supported plate is investigated. The classic and the strain EMA were performed with a piezoelectric accelerometer and the piezoelectric strain gauges, respectively. The results show that the accuracy of the strain EMA results (the natural frequencies, DMSs and the damping) is comparable to the accuracy of the classic EMA.

Keywords: Experimental modal analysis, strain response, the piezoelectric strain sensor, strain mode shapes

1 Introduction

The classic Experimental Modal Analysis (EMA) (Ewins (1984); Maia and Silva (1997); He and Fu (2001); Heylen *et al.* (2007)) is based on an experimental identification of the Frequency Response Functions (FRFs), where the responses are measured with motion sensors (*e.g.*, piezoelectric accelerometer, laser vibrometer) and the excitation is performed with a modal hammer or electrodynamic shaker. The excitation forces are measured with force transducers. The measured FRFs are used for the extraction of the modal parameters with an identification method (*e.g.*, the Ewins-Gleeson method, the Complex Exponential method) (Ewins (1984); Maia and Silva (1997)). The results of the classic EMA are the natural frequencies, the damping and the mass-normalized Displacement Mode Shapes (DMSs); where the term mass normalization is used for the scaling with respect to the orthogonality properties of the mass-normalized modal matrix (Ewins (1984); Maia and Silva (1997)).

The strain EMA (Bernasconi and Ewins (1989a); Yam *et al.* (1996); Bernasconi and Ewins (1989b); Yam *et al.* (1994)) is a special approach in the field of EMA. It is based on an experimental identification of the strain FRFs. The excitations are performed in a similar way as in the classic EMA and the responses are measured with strain sensors. The dynamic strains are usually measured with strain gauges that are attached to the surface of a tested structure with a bond. The strain responses can be measured with several types of strain gauges. For example, in (Bernasconi and Ewins (1989b)), (Cusano *et al.* (2006); Hwang *et al.* (2011)), (Chen and Wang (2004)) and (Kranjc *et al.* (2013)) the strain responses were measured with semiconductor strain gauges, Fiber-Bragg Grating (FBG) sensors, polyvinylidene fluoride films and piezoelectric strain gauges, respectively. The experimentally identified strain FRFs are used for

the modal-parameter identification using the same methods as in the classic EMA (Bernasconi and Ewins (1989a); Yam *et al.* (1996)). The results of the strain EMA are natural frequencies, DMSs, Strain Mode Shapes (SMSs) and damping (Bernasconi and Ewins (1989a); Yam *et al.* (1996)). The identified DMSs and SMSs cannot be mass-normalized (Bernasconi and Ewins (1989a)) only with the strain EMA. When the DMSs and SMSs are not mass-normalized they do not match the numerically calculated DMSs, due to the incorrect scaling (Kranjc *et al.* (2013)). The mass-normalized DMSs are required for the identification of the spatial properties (mass, stiffness and damping matrices) of the dynamical system. The mass normalization in the strain EMA can be performed with the help of the classic EMA (Yam *et al.* (1996)) or with the help of mass-change strategy for the strain EMA (Kranjc *et al.* (2013)). The advantages of the strain EMA are as follows. It enables an experimental investigation of the stress-strain distribution (in contrast to the classic EMA, where numerical/analytical transformations are required). This advantage can be used in the field of vibration fatigue (Mršnik *et al.* (2013); Česnik *et al.* (2012); Wentzel (2013)) where the discrepancies between the stress/strain responses of vibrational-fatigue models and the true values lead to the large errors in the life estimations; therefore, the models have to be validated. This validation can be made using the classic EMA that requires a transformation from the motion to the stress responses. Due to the errors in the transformation, the strain EMA is more suitable for the validation than the classic EMA. As shown in Yam *et al.* (1994), the SMSs are more sensitive to the structural local changes than the DMSs. This advantage can be used for local damage identification at the structurally critical points. The strain EMA can also be used instead of the classic EMA to identify the modal parameters when a motion sensor cannot be used (*e.g.*, the location near the clamped boundary condition with no motion). There is a lack of research regarding a comparison between the strain and the classic EMA. When using the strain EMA instead of the classic EMA for modal-parameter identification, it is important to know the experimental and theoretical differences, and whether the accuracy of the results is the same as for the results of the classic EMA.

The article is organized as follows: In Section 2 the theoretical basics and the differences between the classic and the strain EMA are presented. This is followed by the experimental comparison, where structures of a free-free supported beam and a free-free supported plate are analyzed with both principles in Section 3. The conclusion follows in Section 4.

2 Theoretical background

2.1 The motion response of a dynamical system

The theory of the motion response of a dynamical system can be found in Ewins (1984); Maia and Silva (1997); He and Fu (2001). The motion response is considered on a hysteretically proportionally damped Multiple-Degrees-Of-Freedom (MDOF) system. The spatial model of the system is written as:

$$\mathbf{M} \ddot{\mathbf{x}}(t) + \mathbf{iD} \dot{\mathbf{x}}(t) + \mathbf{K} \mathbf{x}(t) = \mathbf{f}(t) \quad (1)$$

where the spatial properties \mathbf{M} , \mathbf{D} and \mathbf{K} are the mass, the damping and the stiffness matrices, respectively. $\mathbf{x}(t)$ is the vector of the mass positions and $\mathbf{f}(t)$ is the vector of the excitations. In the case of proportional damping, the matrix \mathbf{D} is proportional to \mathbf{M} and (or) \mathbf{K} . The spatial properties of the system can be used for a calculation of the modal parameters of the system. By considering the modal parameters, the motion steady-state response of the hysteretically proportionally damped dynamical system can be written in the frequency domain as:

$$\mathbf{X}(\omega) = \mathbf{\Phi} [\omega_r^2(1 + i\eta_r) - \omega^2]^{-1} \mathbf{\Phi}^T \mathbf{F}(\omega) = \mathbf{H}(\omega) \mathbf{F}(\omega) \quad (2)$$

where $\mathbf{X}(\omega)$ is the motion steady-state response, $\mathbf{\Phi}$ is the modal matrix (matrix of the mass-normalized DMSs), ω_r are the natural frequencies, η_r are the damping loss factors, $\mathbf{F}(\omega)$ is the vector of the excitation force, $\mathbf{H}(\omega)$ is the receptance matrix and $[\]$ denotes a diagonal matrix. An element of the matrix contains the information about the receptance between the structure points j and k , and can be written as:

$$H_{jk}(\omega) = \sum_{r=1}^N \frac{{}_r A_{jk}}{\omega_r^2 - \omega^2 + i\eta_r \omega_r^2} \quad (3)$$

where ${}_r A_{jk} = \phi_{jr} \phi_{kr}$ is the modal constant. There are two important properties of the receptance matrix. First, the principle of reciprocity $H_{jk}(\omega) = H_{kj}(\omega)$, which is known as the symmetry of $\mathbf{H}(\omega)$ and second, the modal constants consistency equations which are described by the following pair of equations:

$${}_r A_{jk} = \phi_{jr} \phi_{kr} \quad (4)$$

$${}_r A_{jj} = \phi_{jr}^2 \quad \text{or} \quad {}_r A_{kk} = \phi_{kr}^2 \quad (5)$$

The importance of Eq. (4) and (5) will be explained in Section 2.3.

2.2 The strain response of a dynamical system

To research the strain response of a dynamical system, the transformation from the displacement to the strain field is introduced. The transformation is performed by applying the operator \mathbf{S} to the displacement field (Bernasconi and Ewins (1989a); Zienkiewicz and Taylor (2005)):

$$\mathbf{S} = \frac{1}{2}(\nabla + \nabla^T) \quad (6)$$

where ∇ is the linear differential operator. To calculate the r -th mass-normalized Strain Mode Shape (SMS) Φ_r^ε , \mathbf{S} is applied to the mass-normalized DMS Φ_r (Bernasconi and Ewins (1989a); Yam *et al.* (1994); Li *et al.* (1989)):

$$\Phi_r^\varepsilon = \mathbf{S}\Phi_r \quad (7)$$

where Φ_r^ε represents the strains corresponding to Φ_r . The strain steady-state response $\mathbf{X}^\varepsilon(\omega)$ of a hysteretically proportionally damped continuous system is obtained by applying the operator \mathbf{S} to the equation of the motion response, Eq. (2) (Bernasconi and Ewins (1989a); Yam *et al.* (1994); Li *et al.* (1989)):

$$\mathbf{X}^\varepsilon(\omega) = \mathbf{S}\mathbf{X}(\omega) = \Phi^\varepsilon [\omega_r^2(1 + i\eta_r) - \omega^2]^{-1} \Phi^T \mathbf{F}(\omega) = \mathbf{H}^\varepsilon(\omega) \mathbf{F}(\omega) \quad (8)$$

where $\mathbf{H}^\varepsilon(\omega)$ is the strain Frequency-Response Function (FRF) matrix and Φ^ε is the matrix of the mass-normalized SMSs. $\mathbf{H}^\varepsilon(\omega)$ can be written as (Yam *et al.* (1996)):

$$\mathbf{H}^\varepsilon(\omega) = \sum_{r=1}^N \frac{{}_r\mathbf{A}^\varepsilon}{\omega_r^2 - \omega^2 + i\eta_r\omega_r^2} \quad (9)$$

where ${}_r\mathbf{A}^\varepsilon$ is the strain modal constants matrix, corresponding to the r -th mode and can be written as:

$${}_r\mathbf{A}^\varepsilon = \begin{bmatrix} \phi_{1r}^\varepsilon\phi_{1r} & \cdots & \phi_{1r}^\varepsilon\phi_{kr} & \cdots & \phi_{1r}^\varepsilon\phi_{N_d r} \\ \vdots & \ddots & \vdots & \ddots & \vdots \\ \phi_{jr}^\varepsilon\phi_{1r} & \cdots & \phi_{jr}^\varepsilon\phi_{kr} & \cdots & \phi_{jr}^\varepsilon\phi_{N_d r} \\ \vdots & \ddots & \vdots & \ddots & \vdots \\ \phi_{N_s r}^\varepsilon\phi_{1r} & \cdots & \phi_{N_s r}^\varepsilon\phi_{kr} & \cdots & \phi_{N_s r}^\varepsilon\phi_{N_d r} \end{bmatrix}_{N_s \times N_d} \quad (10)$$

where ϕ_{jr}^ε and ϕ_{kr} are the components of $\mathbf{\Phi}_r^\varepsilon$ and $\mathbf{\Phi}_r$, respectively. N_d and N_s are the sizes of $\mathbf{\Phi}_r$ and $\mathbf{\Phi}_r^\varepsilon$, respectively. Eq. (10) shows that the strain modal constant matrix is not symmetric (${}_rA_{jk}^\varepsilon \neq {}_rA_{kj}^\varepsilon$); therefore, $H_{jk}^\varepsilon \neq H_{kj}^\varepsilon$. \mathbf{H}^ε is, in general, not a square matrix (Yam *et al.* (1996)).

2.3 The identification of the modal parameters with the classic approach

The classic EMA (Ewins (1984); Maia and Silva (1997); He and Fu (2001)) is one of the most frequently used procedures for the experimental identification of modal parameters; therefore, only the details that are important to this research are presented. When considering the proportional hysteretic damped structure, the results of an indirect identification method (*e.g.*, the Ewins-Gleeson identification method) are the natural frequencies, the damping loss factors and the modal constants. The modal constants that are identified from the j -th row and the k -th column of the motion-FRF matrix, denoted as ${}_r\mathbf{A}_j = \phi_{jr} \mathbf{\Phi}_r$ and ${}_r\mathbf{A}_k = \mathbf{\Phi}_r \phi_{kr}$, respectively, contain the information about the DMSs.

The mass-normalization of DMSs: To obtain the mass-normalized DMSs, the normalization procedure (for details, see Ewins and Gleeson (1982)) has to be performed by taking into account the modal constants consistency equations (Eq. (4) and (5)). A direct motion FRF (accelerance, mobility or receptance) is measured by exciting the structure and measuring the motion response at the same location ($j = k$). From the direct FRF the modal constants ${}_rA_{jj} = \phi_{jr}^2$ (${}_rA_{kk} = \phi_{kr}^2$) are identified and used for the calculation of the j -th (k -th) components of the mass-normalized DMSs ϕ_{jr} (ϕ_{kr}). The mass-normalized DMSs $\mathbf{\Phi}_r$ are calculated using the following equation:

$$\mathbf{\Phi}_r = \pm \frac{{}_r\mathbf{A}_j}{\phi_{jr}} = \pm \frac{{}_r\mathbf{A}_k}{\phi_{kr}} \quad (11)$$

In general, the sign of $\mathbf{\Phi}_r$ can be positive or negative.

2.4 The strain EMA

The strain EMA (Bernasconi and Ewins (1989a); Yam *et al.* (1996)) is similar to the classic EMA. During the modal testing the structure is excited with a known force at the point k and the response is measured with a strain sensor at the point j . The time signals of the excitation and the strain response are used

for an estimation of the strain FRF (H_{jk}^ε) using the FRF estimators (Maia and Silva (1997)) for the classic EMA. The strain EMA can be done in a way so as to identify the DMSs and SMSs (see Fig. 1).

To identify the DMSs the strain FRFs are measured in such a way that the strain-response measurement point j is fixed and the structure is excited at the points $1 - N_d$ (see Fig. 1). The results of the modal testing are strain FRFs that belong to the j -th row of the strain FRF matrix: $H_{j1}^\varepsilon, \dots, H_{jN_d}^\varepsilon$. The modal parameters are identified with the methods that were originally developed for the classic EMA. When an indirect identification method is used, the natural frequencies ω_r , the strain modal constants ${}_r A_{jk}^\varepsilon$ and the damping are identified from each measured H_{jk}^ε . From the row of the strain FRF matrix the j -th row of the matrix of strain modal constants is identified: ${}_r A_{j1}^\varepsilon, \dots, {}_r A_{jN_d}^\varepsilon$. It can be written as:

$${}_r \mathbf{A}_j^\varepsilon = \phi_{jr}^\varepsilon \mathbf{\Phi}_r \quad (12)$$

Eq. (12) shows that the strain modal constants, that are identified from the row of \mathbf{H}^ε , contain the information about the DMSs. The identification of the SMSs is done in a similar way as the identification of the DMSs. During the modal testing, the strain FRFs are measured in such a way that the excitation point k is fixed and the strain response is measured at the points $1 - N_s$. The results of the modal testing are the strain FRFs that are in the k -th column of the strain FRF matrix: $H_{1k}^\varepsilon, \dots, H_{N_s k}^\varepsilon$. From each measured strain FRF the natural frequencies, the strain modal constants and the damping are identified. The identified strain modal constants are the k -th column of the strain modal constant's matrix: ${}_r A_{1k}^\varepsilon, \dots, {}_r A_{N_s k}^\varepsilon$. It can be written as:

$${}_r \mathbf{A}_k^\varepsilon = \mathbf{\Phi}_r^\varepsilon \phi_{kr} \quad (13)$$

Eq. (13) shows that the strain modal constants that are identified from the column of \mathbf{H}^ε contain the information about the SMSs.

The mass-normalization of DMSs and SMSs: It is clear from Eq. (10) that the consistency equations (Eq. (4) and (5)) are not valid for the strain modal constants. The strain modal constants that are identified from the direct strain FRF (excitation and the response at the same structure point ($j = k$)), denoted as ${}_r A_{jj}^\varepsilon = \phi_{jr}^\varepsilon \phi_{jr}$, are not the square of mass-normalized DMS components ϕ_{jr} as in the classic EMA (see section 2.3); therefore, the mass-normalization (scaling procedure) of the DMSs and SMSs cannot be performed with the strain EMA (Bernasconi and Ewins (1989a); Yam *et al.* (1996)).

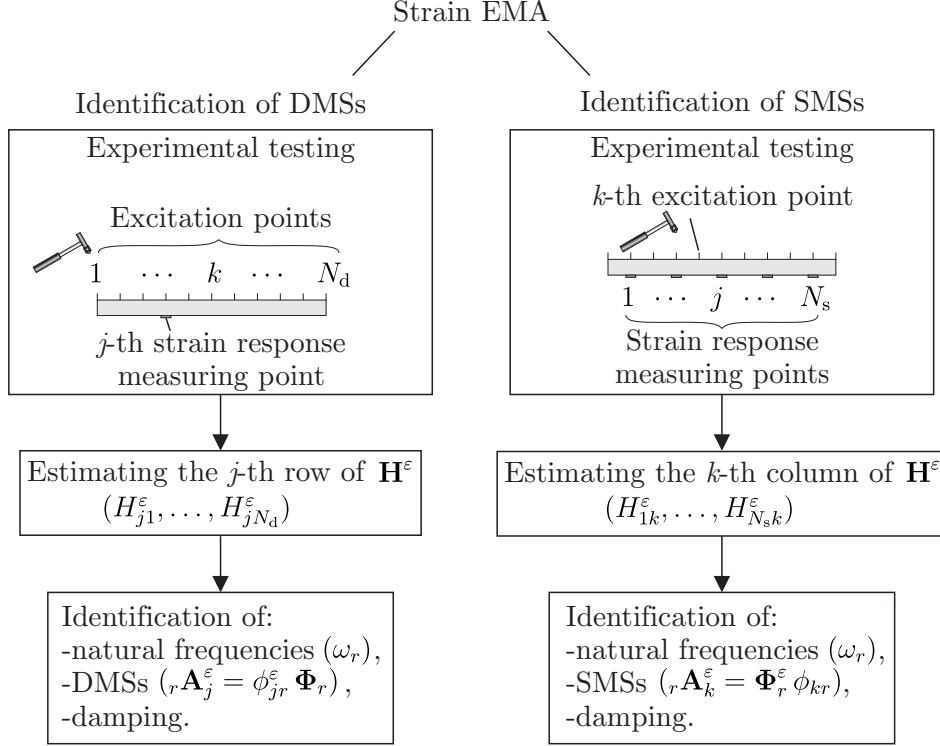


Fig. 1: The strain EMA

The mass-normalization can be performed with the help of the classic EMA that requires the use of a motion sensor. A direct motion FRF is measured at the point k and used to identify the k -th components of Φ_r (see Section 2.3) denoted as ${}_{\text{EMA}}\phi_{kr}$. The subscript ${}_{\text{EMA}}$ indicates that ${}_{\text{EMA}}\phi_{kr}$ is identified using the classic EMA. The mass-normalization of the DMSs and SMSs is performed using the following equations:

$$\Phi_r = \pm \frac{{}_r\mathbf{A}_j^e {}_{\text{EMA}}\phi_{kr}}{{}_rA_{jk}^e} \quad (14)$$

$$\Phi_r^e = \pm \frac{{}_r\mathbf{A}_k^e}{{}_{\text{EMA}}\phi_{kr}} \quad (15)$$

Regarding the sign of Φ_r in Eq. (14), the same comment is valid as for Eq. (11). If one would like to identify Φ_r^e , that are orientated corresponding to Φ_r , the signs in Eq. (14) and Eq. (15) have to be the same.

The mass normalization can also be performed with the mass-change strategy for the strain EMA (Kranjc *et al.* (2013)), which is based on the structure modification by mass adding.

3 Experimental comparison of the strain and the classic EMA

The comparison between the classic and the strain EMA was performed on structures of a beam and a plate.

3.1 The measurement equipment

During the modal testing the responses are measured with a piezoelectric accelerometer (B&K-4508 B 001) and a piezoelectric strain gauge (PCB 740B02). The excitations are performed with a modal hammer (B&K-8206). Since in the field of structural dynamics, the piezoelectric accelerometer and the modal hammer are well known, here we will only provide more details about the piezoelectric strain gauge.

The piezoelectric strain gauge is described in Dosch (1999) and Rovšček *et al.* (2012). It consists of a quartz sensing element and microelectronic signal conditioning, which are integrated into a titanium housing (see Fig. 2). The dimensions of the sensor are $5.1 \times 15.2 \times 1.8$ mm. The sensor uses a two-wire direct-current power supply (ICP[®]). The sensitivity of each sensor is calibrated before it is shipped to the customer. The sensor is attached to the test structure by an adhesive bond. An inappropriate attachment of the sensor can change the sensor's sensitivity. To achieve accurate measurements the attaching has to be performed carefully in accordance with the manufacturer's instructions.

One of the important characteristics of the sensor is its ability to resolve extremely small strain signals. The broadband noise floor of the sensor is $0.0006 \mu\varepsilon$. The measurements are accurate when the wavelength of the stress in a tested structure is large compared to the length of the sensor. The manufacturer proposes that the wavelength of the stress should be at least ten times the length of the sensor. The strain measurement frequency limit for steel (regarding the wavelength) is approximately 33.6 kHz. The inherent transverse sensitivity of the sensor is equal to -1.9% and the sensitivity to the in-plane shear strain is zero.

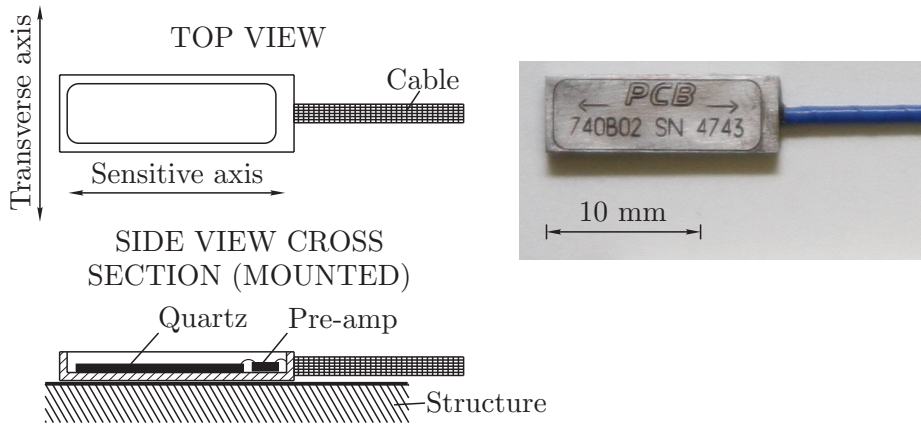


Fig. 2: The piezoelectric strain gauge PCB 740B02

3.2 Experimental testing on the beam

The first experimental testing was performed on a $1 \text{ m} \times 0.03 \text{ m} \times 0.01 \text{ m}$ steel beam. As shown in Fig. 3, 11 equally spaced points were chosen, at which the components of the DMSs are identified (the components of the SMSs are identified only at the points 2,4,6,8,10) using the strain and the classic EMA. Only the first five bending modes around the z -axis were considered; these result in displacements in the y -axis and normal strains in the x -axis. The boundary conditions of the structure were free-free, which were achieved by suspending the beam from two elastic strings. The strings were attached at the nodes of the first DMS (near the structure points 3 and 9). The structure vibrated transversely to the strings and the natural frequencies of the motion rigid modes were low in comparison to the structure's first natural frequency; therefore, the effects of the attaching are negligible. To make the comparison, both the classic and the strain EMA were performed.

3.2.1 The classic EMA

To identify the modal parameters with the classic EMA the modal testing was performed with the response being measured by the accelerometer at point 1 (Fig. 3), while the structure was excited with the modal hammer at the points 1-11 (the row of the accelerance matrix was measured). The response was measured at the point where the deflections corresponding to each of the first five modes are significant. The tested structures are considered as lightly damped;

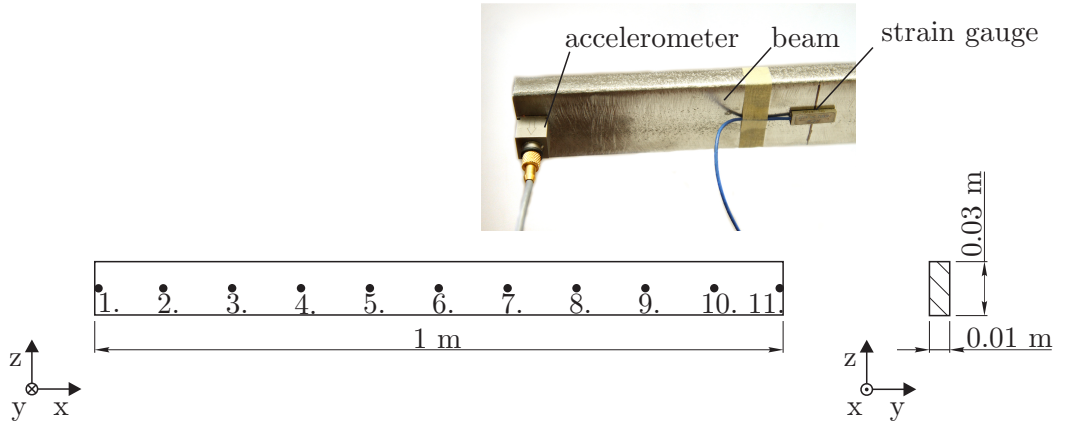


Fig. 3: The tested beam

therefore, the modal-parameter identification was performed with the Ewins-Gleeson method (Ewins and Gleeson (1982)). This method is used for the identification of lightly damped structures (the tested structure is lightly damped) assuming the hysteretic damping model. The authors of the method consider that the DMSs of such structures are real (with phase shifts of 0 or 180 degrees). With the classic EMA the natural frequencies, the mass-normalized DMS and the damping loss factors of the beam were identified. The classic EMA results are considered in Section 3.2.3.

3.2.2 The strain EMA

The strain gauges were attached at the points 2, 4, 6, 8 and 10. To obtain the information about the modal parameters with the strain EMA, the strain response was measured at the point 8 (Fig. 3), where the strains corresponding to each of the first five modes are significant. The excitations were performed in the same way as in the classic EMA (Section 3.2.1). The measured strain FRFs are the row of the strain FRF matrix. To show how it is possible for the strain EMA to identify the SMSs, the responses were measured at the points 2, 4, 6, 8 and 10, while the structure was excited at the point 1. The measured strain FRFs are the column of the strain FRF matrix. The natural frequencies, the strain modal constants and the damping loss factors were identified with the same identification method as in the classic EMA (Section 3.2.1). The accuracy of the modal identification was analyzed by the strain FRF reconstructions. An example of the reconstruction is shown in Fig. 4, where the reconstructed

H_{88}^ε (the strain FRF between the response and the excitation at the point 8) is plotted together with the measured one. Fig. 4 shows that the reconstructed H_{88}^ε is in good agreement with the measured one.

From the strain modal constants the DMSs (${}_r\mathbf{A}_{j=8}^\varepsilon$) and SMSs (${}_r\mathbf{A}_{k=1}^\varepsilon$) were obtained (see Section 2.4). The identified DMSs and SMSs are plotted in Fig. 5 together with the shapes that were calculated with the ANSYS Finite-Element Method (FEM) software. The finite-element model was built from 0.01 m-long BEAM189 elements. The mass normalization of the shapes cannot be performed with the strain EMA (Section 2.4) only; therefore, the shapes in Fig. 5 are normalized by making the largest peak or valley of the DMSs and SMSs equal to unity. The figure shows that the experimentally identified DMSs (Fig. 5(a-e)) and SMSs (Fig. 5(f-j)) match the calculated ones well. The identified natural frequencies and the damping loss factors can be found in Section 3.2.3.

Attaching the strain sensor in a way that is not in accordance with the manufacturer's instructions can result in changes to the sensor's sensitivity. However, the changed sensitivity does not affect the accuracy of the identified natural frequencies, the damping loss factors and the DMSs (see Eq. (9) and (10)). The sensitivity changes affect the accurate identification of the SMSs.

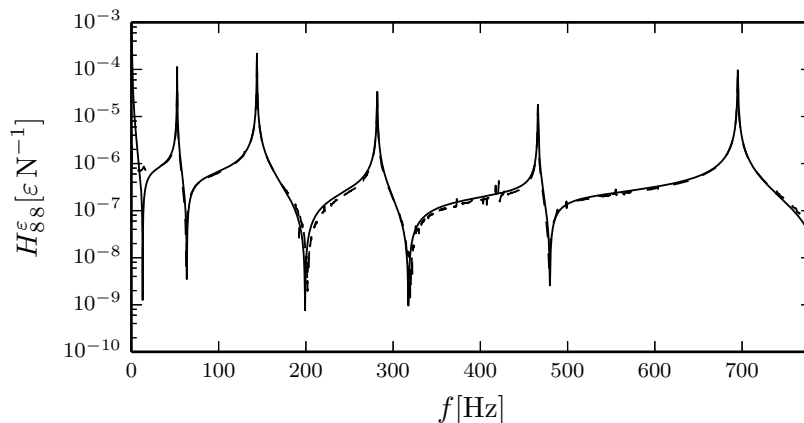


Fig. 4: The measured (- - -) and the reconstructed (—) strain FRF

3.2.3 The comparison of the classic and strain EMA results

The results of the strain EMA were compared to the results of the classic EMA. First, the natural frequencies were compared. This comparison showed that the

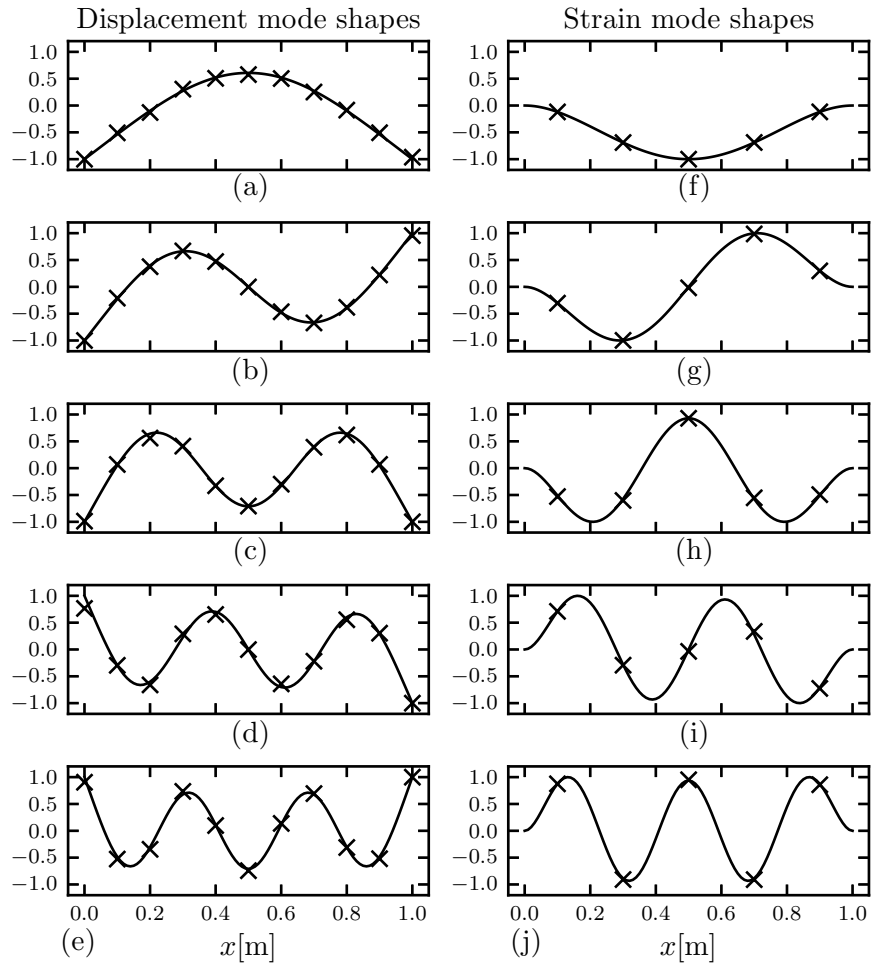
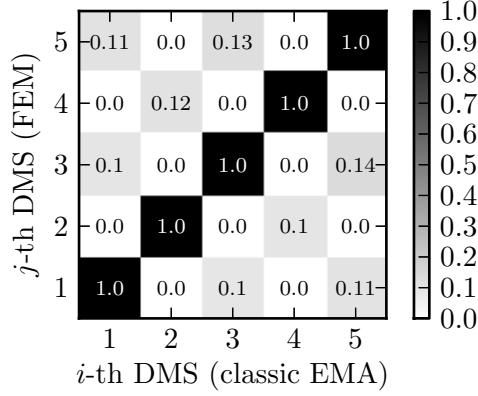


Fig. 5: The identified (\times) and the calculated ($—$) DMSs and SMSs

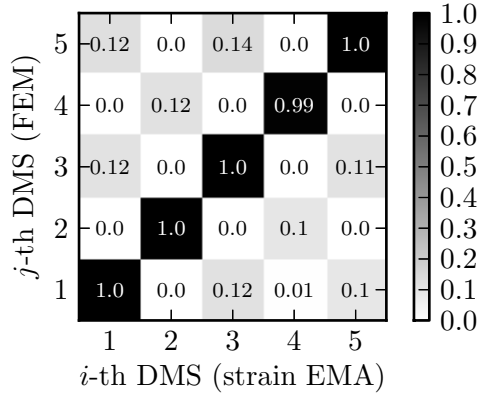
natural frequencies that were identified from the strain FRFs and the accelerances have the same values at the frequency resolution of 0.1 Hz. They occur at 52.4 Hz, 143.9 Hz, 281.7 Hz, 465.8 Hz and 694.9 Hz.

Next, the comparison of the DMSs followed. This was performed by a Modal Assurance Criterion analysis (MAC) (Allemang (2003)), where the identified DMSs (the results of the classic and the strain EMA) were compared to the calculated values using the FEM. The DMSs, that were identified with the classic and the strain EMA are compared to the calculated ones in Fig. 6(a) and Fig. 6(b), respectively. The MAC analysis shows that the DMSs that were

identified with the strain and classic EMA are in good agreement with the calculated DMSs. A comparison of Fig. 6(a) and 6(b) shows that the accuracy of the identified DMSs is approximately the same for both methods.



(a)



(b)

Figure 6: MAC comparison of the identified DMSs and the calculated ones; (a) results of the classic EMA, (b) results of the strain EMA

Finally, a comparison of the damping was made. This involved comparing the average damping loss factors that were identified from the measured accelerances (denoted as $\tilde{\eta}_r$) and the strain FRFs, where the response was measured at the point 8 (denoted as $\tilde{\eta}_r^\varepsilon$). The highest and the lowest values of the damping loss factors were not considered in the calculation. The comparison is shown in Tab. 1, where δ_η are the relative deviations between $\tilde{\eta}_r^\varepsilon$ and $\tilde{\eta}_r$. Tab. 1 shows that $\tilde{\eta}_r^\varepsilon$ and $\tilde{\eta}_r$ are approximately the same, with the highest deviation being

5 %.

Table 1: Comparison of the η_r that were identified with the strain and the classic EMA for the beam

r	$\tilde{\eta}_r^\varepsilon$	$\tilde{\eta}_r$	δ_η
1	0.002210	0.002187	1.1 %
2	0.001171	0.001191	-1.6 %
3	0.001138	0.001137	0.1 %
4	0.000575	0.000548	5.0 %
5	0.000511	0.000493	3.7 %

3.3 Experimental testing on the plate

The second experimental test was performed on the $0.4 \text{ m} \times 0.32 \text{ m} \times 0.03 \text{ m}$ steel free-free supported plate. As shown in Fig. 7, 6×5 equally spaced points were chosen (points 1-30) where the components of the DMSs will be identified. The free-free boundary conditions were achieved in a similar way as in the case of the beam by suspending the structure from two elastic strings. The attachment points of the strings are shown in Fig. 7. Only the first five modes were considered; these vibrate out of the xy -plane and result in normal and shear strains (stresses) (see Leissa (1969)). The same measurement equipment was used as in the case of the beam. To make the comparison, both the classic and the strain EMA were performed.

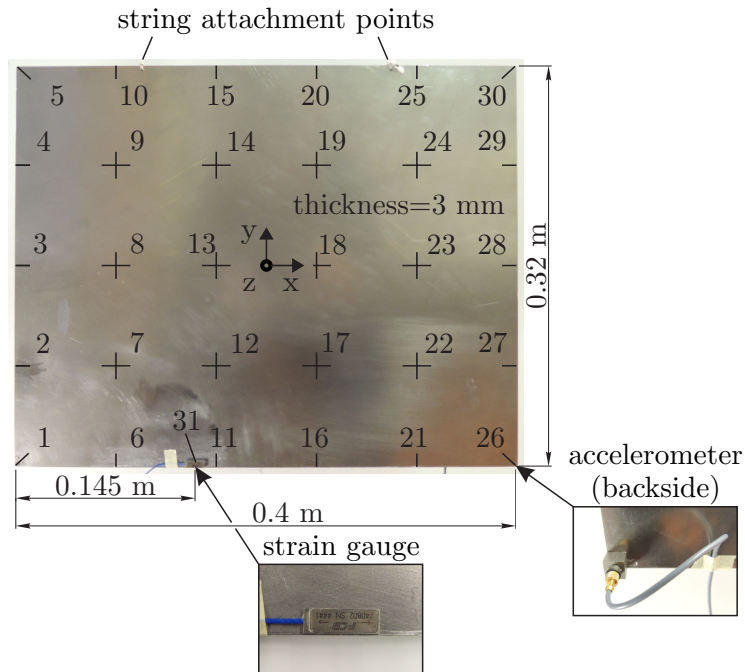


Fig. 7: The plate structure

3.3.1 The classic and the strain EMA

To obtain the information about the DMSs with the classic EMA the motion response was measured at the point 26 (Fig. 7), while the structure was excited with the modal hammer at the points 1-30. To obtain the information about the DMSs with the strain EMA the normal- x -component of the strain response was measured at the point 31 and the structure was excited in the same way as in the classic EMA. The sensors (accelerometer and strain gauge) were attached at the points where the responses (motion and x -component of strain) corresponding to each of the first five modes are significant. The modal-parameter identification was performed with the same identification method as in the case of the beam. The identification was validated by FRF reconstructions. The example of the reconstruction is shown for the strain FRF between the points 31 (response) and 26 (excitation) $H_{31\ 26}^\varepsilon$ (Fig. 8). Fig. 8 shows that the reconstructed and the measured strain FRFs are in good agreement. The DMSs that were identified with the strain EMA ($r\mathbf{A}_{j=31}^\varepsilon$) are plotted in Fig. 9 together with the calculated ones using the FEM. The calculation was made with Ansys software, where the finite-element model was built from $0.008\text{ m} \times 0.008\text{ m}$ -sized SHELL181 elements. The mode shapes are scaled to unity in a similar way as in Fig. 5. Fig. 9(a)-(e) show the comparison of the DMSs components for all the measuring points. Fig. 9(f)-(j) show a detailed comparison at the location $y=-0.08\text{ m}$. Fig. 9 shows that the DMSs that are identified with the strain EMA are in good agreement with the calculated ones. The remaining results of the strain EMA and the classic EMA are considered in Section 3.3.2.

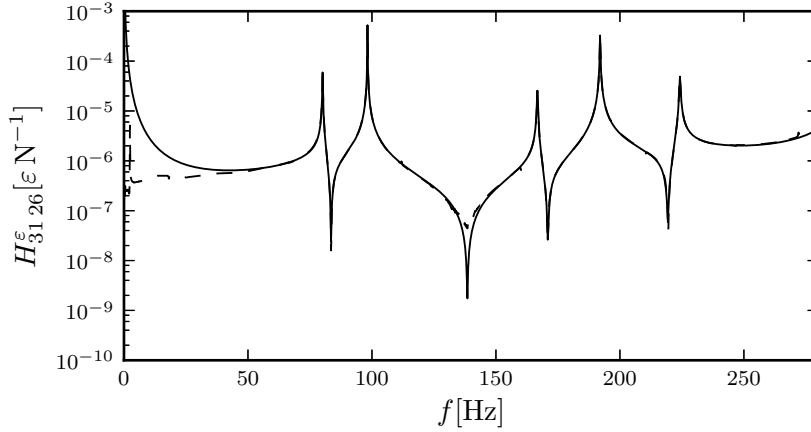


Fig. 8: The measured (---) and the reconstructed (—) strain FRF

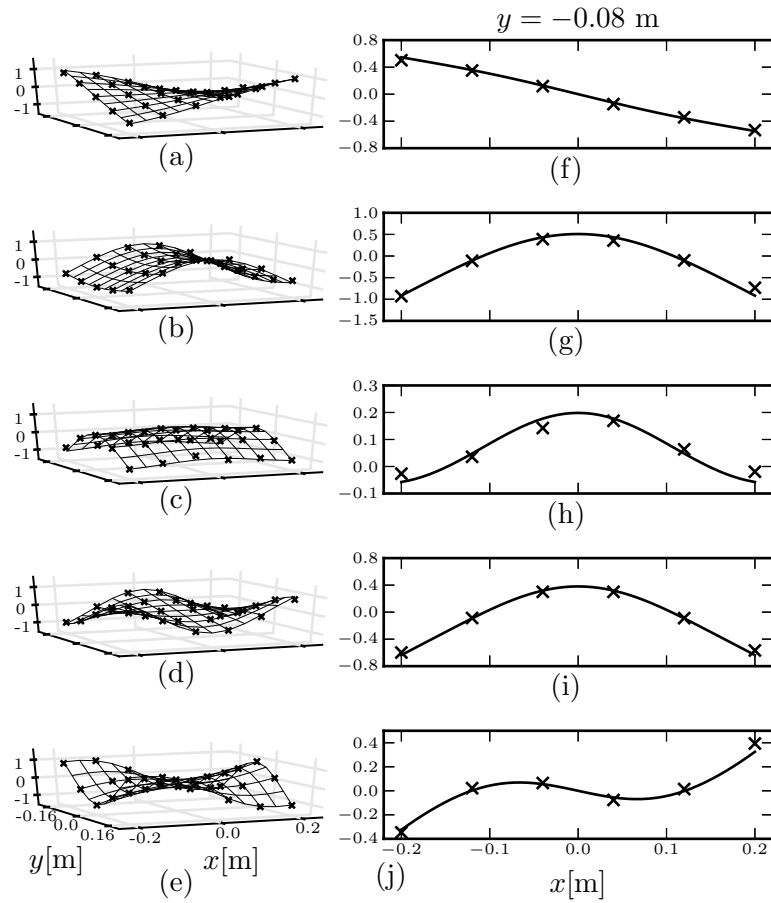
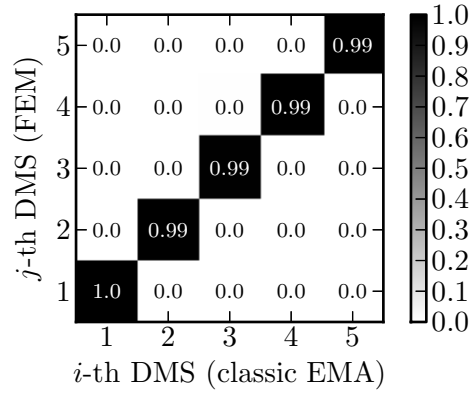


Fig. 9: The identified (—) and the calculated (\times) DMSs

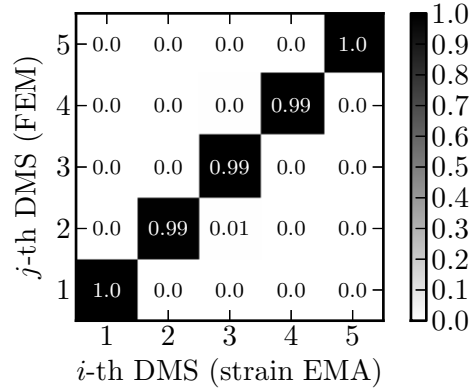
3.3.2 The comparison of the results

The results were compared in a similar way as in the case of the beam. First, the identified natural frequencies were compared. The identical values of the natural frequencies were identified with the classic and the strain EMA. The natural frequencies occur at 80.1 Hz, 98.2 Hz, 166.7 Hz, 192 Hz and 224.2 Hz. The frequency resolution of the results is 0.1 Hz. What follows is a comparison of the DMSs with the MAC analysis. The DMSs, that were identified with the classic EMA and the strain EMA are compared to the calculated ones by FEM in Fig. 10(a) and Fig. 10(b), respectively. Fig. 10 shows that the identified

DMSs accurately match the calculated ones and that approximately the same accuracy was achieved with both principles. Finally, the comparison of the damping was made. It was performed in a similar way as in the case of the beam. The average damping loss factors were calculated from the FRFs where the highest and the lowest five values were not considered in the calculation. The comparison is shown in Tab. 2. Tab. 2 shows that approximately identical damping loss factors were identified with the classic and the strain EMA. The largest deviation is less than 4 %.



(a)



(b)

Figure 10: MAC comparison of the identified DMSs and the calculated ones; (a) result of the classic EMA, (b) result of the strain EMA

Table 2: The comparison of the η_r , that were identified with the strain and the classic EMA for the plate

r	$\tilde{\eta}_r^\varepsilon$	$\tilde{\eta}_r$	δ_η
1	0.001455	0.001514	-3.9 %
2	0.000637	0.000635	0.4 %
3	0.001496	0.001549	-3.5 %
4	0.000832	0.000847	-1.7 %
5	0.001506	0.001501	0.4 %

4 Conclusion

In this research two approaches to the identification of the structure's modal parameters were compared. In the field of structural dynamics the modal parameters of the real structures are usually identified with the classic Experimental Modal Analysis (EMA). The less-known strain EMA is a special approach in the field of EMA that can be used to identify the natural frequencies, the damping of the Displacement Mode Shapes (DMSs) and the Strain Mode Shapes (SMSs). The advantages of the strain EMA are that it can be used for an experimental investigation of the stress-strain distribution, which is important for the analysis of the vibration fatigue and the damage identification. It can also be used instead of the classic EMA for the identification of the modal parameters. The mass-normalization of the DMSs and SMSs cannot be performed with the strain EMA only.

In this article we looked at whether the results of the strain EMA can be compared to the results of the classic EMA. The experimental tests were performed in such a way that, during the modal testing, the responses were measured with a piezoelectric accelerometer and piezoelectric strain gauges. The strain and the classic EMA were performed on the beam and the plate structures. The results of the testing were the natural frequencies, the DMSs and the damping loss factors. To show the additional application possibility of the strain EMA, the SMSs of the beam were also identified.

The comparison of the experimental results showed the following: First, identical natural frequencies were identified with both principles. Next, the quality of the identified DMSs (not mass-normalized) is the same for both principles and, finally, both principles give approximately the same values for the damping loss factors.

The research showed that the strain EMA can be used instead of the classic

EMA for an accurate identification of the natural frequencies, the displacement mode shapes and the damping, when the appropriate measuring equipment is used.

Acknowledgement

The operation was partially Financed by the European Union, European Social Fund (grant nr. P-MR-10/137).

References

- Allemang RJ (2003) The modal assurance criterion - Twenty years of use and abuse. *Sound and Vibration* 37(8): 14–23.
- Bernasconi O and Ewins DJ (1989a) Modal strain/stress fields. *The International Journal of Analytical and Experimental modal analysis* 4(2): 68–76.
- Bernasconi O and Ewins DJ (1989b) Application of strain modal testing to real structures. Proceedings of the 7th International Modal Analysis Conference (IMAC-VII) 1453–1464.
- Chen RL and Wang BT (2004) The use of polyvinylidene fluoride films as sensors for the experimental modal analysis of structures. *Smart Materials and Structures* 13(4): 791–799.
- Cusano A and Capoluongo P and Campopiano S and Cutolo A and Giordano M and Felli F and Paolozzi A and Caponero M (2006) Experimental modal analysis of an aircraft model wing by embedded fiber Bragg grating sensors. *Sensors Journal, IEEE* 6(1): 67–77.
- Česník M and Slavič J and Boltežar M (2012) Uninterrupted and accelerated vibrational fatigue testing with simultaneous monitoring of the natural frequency and damping. *Journal of Sound and Vibration* 331(24):5370–5382.
- Dosch JJ (1999) Piezoelectric strain sensor. *Proceedings of the 17th International Modal Analysis Conference (IMAC-XVII)* 537–542.
- Ewins DJ and Gleeson PT (1982) A method for modal identification of lightly damped structures. *Journal of Sound and Vibration* 84(1): 57–79.
- Ewins DJ (1984) *Modal Testing: Theory and Practice*. Research Studies Press, John Wiley and Sons, Lechtworth, New York etc.

- He J and Fu ZF (2001) *Modal Analysis*. Butterworth-Heinemann, Oxford, Boston etc.
- Heylen W and Lammers S and Sas P (2007) *Modal Analysis Theory and Testing*. Haverlee: Katholieke Universiteit Leuven.
- Hwang GS and Ma CC and Huang DW (2011) Dynamic strain measurements of a cantilever using the improved bonding fiber Bragg grating. *Journal of Vibration and Control* 17:2199–2212.
- Kranjc T and Slavič J and Boltežar M (2013) The mass normalization of the displacement and strain mode shapes in a strain experimental modal analysis using the mass-change strategy. *Journal of Sound and Vibration* 332(26): 6968-6981
- Leissa AW (1969) *Vibration of plates*. NASA SP-160 US Government Printing Office
- Li D and Zhuge H and Wang B (1989) The principle and techniques of experimental strain modal analysis. *Proceedings of the 7th International Modal Analysis Conference (IMAC-VII)* 1285–1289.
- Maia NMM and Silva JMM (1997) *Theoretical and Experimental Modal Analysis*. Research Studies Press, John Wiley and Sons, Taunton, New York etc.
- Mršnik M and Slavič J and Boltežar M (2013) Frequency-domain methods for a vibration-fatigue-life estimation - Application to real data. *International Journal of Fatigue* 47(0):8–17.
- Rovšček D and Slavič J and Boltežar M (2012) The use of strain sensors in an experimental modal analysis of small and light structures with freefree boundary conditions. *Journal of Vibration and Control* 19(7): 1072-1079
- Yam LY and Leung TP and Li DB and Xue KZ (1996) Theoretical and experimental study of modal strain analysis. *Journal of Sound and Vibration* 191(2): 251–260.
- Yam LY and Li DB and Leung TP and Xue KZ (1994) Experimental study on modal strain analysis of rectangular thin plates with small holes. *Proceedings of the 12th International Modal Analysis Conference (IMAC-XII)* 1415–1421.
- Wentzel H (2013) Fatigue test load identification using weighted modal filtering based on stress. *Mechanical Systems and Signal Processing* Epub ahead of print 6 July 2013. DOI:10.1016/j.ymssp.2013.06.014

Zienkiewicz OC and Taylor RL (2005) *The Finite Element Method Set*. Elsevier Science.